

# Substitutions in the redox-sensing PAS domain of the NifL regulatory protein define an inter-subunit pathway for redox signal transmission

Richard Little,<sup>1</sup> Paloma Salinas,<sup>1†</sup> Peter Slavny,<sup>1‡</sup>  
Thomas A. Clarke<sup>2</sup> and Ray Dixon<sup>1\*</sup>

<sup>1</sup>Department of Molecular Microbiology, John Innes Centre, Norwich Research Park, Norwich NR4 7UH, UK.

<sup>2</sup>School of Biological Sciences, University of East Anglia, Norwich Research Park, Norwich NR4 7TJ, UK.

## Summary

The Per-ARNT-Sim (PAS) domain is a conserved  $\alpha\beta$  fold present within a plethora of signalling proteins from all kingdoms of life. PAS domains are often dimeric and act as versatile sensory and interaction modules to propagate environmental signals to effector domains. The NifL regulatory protein from *Azotobacter vinelandii* senses the oxygen status of the cell via an FAD cofactor accommodated within the first of two amino-terminal tandem PAS domains, termed PAS1 and PAS2. The redox signal perceived at PAS1 is relayed to PAS2 resulting in conformational reorganization of NifL and consequent inhibition of NifA activity. We have identified mutations in the cofactor-binding cavity of PAS1 that prevent ‘release’ of the inhibitory signal upon oxidation of FAD. Substitutions of conserved  $\beta$ -sheet residues on the distal surface of the FAD-binding cavity trap PAS1 in the inhibitory signalling state, irrespective of the redox state of the FAD group. In contrast, substitutions within the flanking A' $\alpha$ -helix that comprises part of the dimerization interface of PAS1 prevent transmission of the inhibitory signal. Taken together, these results suggest an inter-subunit pathway for redox signal transmission from PAS1 that propagates from core to the surface in a conformation-dependent manner requiring a flexible dimer interface.

## Introduction

PAS (Per-ARNT-Sim) domains play a key role in signal transduction in all kingdoms of life by detecting environmental parameters via bound co-factors, sensing various small molecules as ligands, in addition to mediating protein–protein interactions. PAS domains have low pairwise sequence identity but possess a highly conserved  $\alpha\beta$  tertiary fold comprised of approximately 110 amino acids in which a central five-stranded anti-parallel  $\beta$ -sheet comprises the most structurally conserved portion of the domain (Taylor and Zhulin, 1999). The central  $\beta$ -sheet of the PAS core has been shown to have a key role in propagating the signal detected by the sensory module. Many PAS domains possess  $\alpha$ -helices that flank the core PAS fold at the amino and/or carboxyl termini. Evidence to date suggests that such flanking helices either extend outwards from the PAS core or pack against the outer surface of the conserved  $\beta$ -sheet. These flanking regions have been implicated in signal transduction from the PAS core to effector domains via  $\alpha$ -helical or coiled coil linkers (Möglich *et al.*, 2009). These recurring features of PAS domains point towards common signalling principles, although the structural plasticity and functional diversity of these signalling modules impose distinctive mechanistic features in diverse examples.

The cytosolic PAS-containing protein NifL, from the diazotrophic bacterium *Azotobacter vinelandii*, provides a model for understanding the mechanism of redox sensing by PAS domains. The function of NifL (a non-catalytic histidine kinase-like protein) in negatively regulating transcription of *nif* genes through interaction with the transcriptional activator NifA has been extensively characterized. NifL inhibits the transcriptional activity of NifA by direct interaction in response to elevated levels of fixed nitrogen and oxygen (Dixon and Kahn, 2004; Martinez-Argudo *et al.*, 2004). Inhibition of NifA prevents wasteful production of the oxygen-sensitive nitrogenase enzyme under conditions whereby nitrogen fixation is either unnecessary or unsustainable. *A. vinelandii* NifL contains two PAS domains in tandem; the N-terminal domain, denoted PAS1, contains a FAD cofactor that senses the redox-status and when oxidized potentiates the formation of the

Accepted 15 August, 2011. \*For correspondence. E-mail ray.dixon@jic.ac.uk; Tel. (+44) 1603 450747; Fax (+44) 1603 450778. †Present address: División de Genética, Universidad de Alicante Apdo. 99 03080 Alicante, Spain. ‡Present address: Department of Biochemistry, University of Cambridge, Cambridge CB2 1QW, UK.

inhibitory conformer of NifL (Hill *et al.*, 1996; Macheroux *et al.*, 1998). The second PAS domain, denoted PAS2, does not apparently bind a cofactor but undergoes quaternary structural changes in response to the redox state of PAS1. This facilitates transmission of the signal to the C-terminal region of the NifL responsible for interaction with NifA (Slavny *et al.*, 2010).

The crystal structure of the oxidized form of the NifL PAS1 domain provides important mechanistic clues into the redox signalling mechanism (Key *et al.*, 2007). A hydrogen-bonding network is present between the isoalloxazine ring structure of FAD and neighbouring amino acids involving two water molecules that are accommodated within an intervening cavity. It has been suggested that reorganization of the hydrogen bonds within the cavity occurs during redox-mediated signalling. The structure is similar to that of other PAS domains and is dimeric in the asymmetric unit with an N-terminal amphipathic helix (N-cap) providing a major part of the dimerization interface (Key *et al.*, 2007). We have utilized the structure of the oxidized PAS1 dimer to guide selection of amino acid substitutions adjacent to the water-filled cavity, within the conserved  $\beta$ -sheet and at the  $\alpha$ -helical dimerization interface. Our combined genetic and biochemical approach reveals a structurally consistent pathway for signal transmission from the core of PAS1 to the surface of the domain in which the dimerization interface plays a key role in the mechanism.

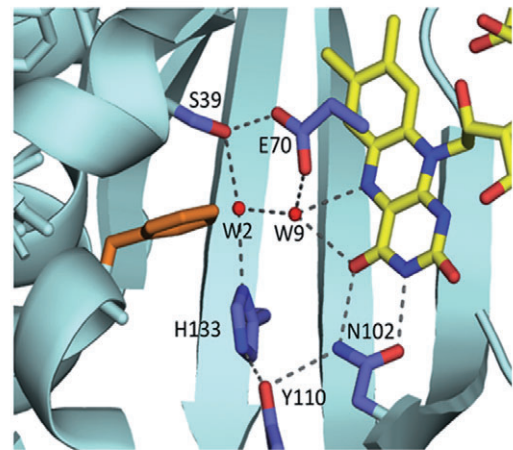
## Results

### Mutagenesis of the FAD binding cavity

The FAD group of NifL is accommodated within a spatially conserved cleft of the PAS1 domain formed by the inner surface of the  $\beta$ -sheet and  $\alpha$ -helices E and F. The redox-active isoalloxazine ring of the oxidized FAD group contributes to an extensive hydrogen bonding network involving two internal water molecules and the side-chains of neighbouring amino acid residues that line the internal cavity (Fig. 1A). Changes in the redox state of FAD are predicted to cause a re-arrangement of the hydrogen-bonding interactions that may in turn be integrated by the participating residues flanking the water-filled cavity, as a steric reorganization. Movement of these residues may therefore provide a mechanism by which redox changes can be perceived as structural signal that can be propagated through the domain (Key *et al.*, 2007).

We reasoned that by making non-conservative substitutions of the flanking residues, we would disrupt the hydrogen-bonding network. Measuring the activity of NifL cavity-mutants in the reduced and oxidized states *in vivo* would therefore allow us to test the importance of this network to redox signal transmission. Residues S39,

A



B

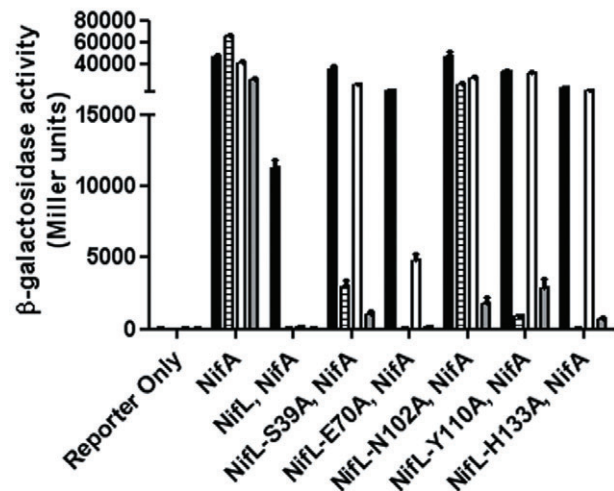


**Fig. 1.** Influence of substitutions in the FAD binding cavity of the NifL PAS1 domain on redox signal transmission.

A. The H-bonding network within the FAD cavity in the oxidized form of NifL, showing the residues lining the cavity as stick models and the internal water molecules Wat2 (W2) and Wat9 (W9) as spheres (Key *et al.*, 2007). The C atoms of the FAD are coloured yellow. F54, which gates the access tunnel, is shown in orange. B. Effect of substitutions on the ability of NifL to regulate transcriptional activation by NifA *in vivo*. Cultures were grown under the following conditions; anaerobically under nitrogen-limiting conditions with casein hydrolysate as the sole nitrogen source (black bars), anaerobically with  $(\text{NH}_4)_2\text{SO}_4$  as nitrogen source (horizontally striped bars), aerobically with casein hydrolysate as the sole nitrogen source (white bars) and aerobically with  $(\text{NH}_4)_2\text{SO}_4$  as nitrogen source (grey bars). Cultures were assayed for  $\beta$ -galactosidase activity as a reporter of NifA-mediated transcriptional activation from the *nifH<sub>2</sub>-lacZ* fusion on plasmid pRT22 as described previously (Slavny *et al.*, 2010). All experiments were performed at least in duplicate with error bars denoting the standard error of the mean.

N102, Y110 and H133 that flank the FAD-binding cavity and contribute to the hydrogen-bonding network were substituted with alanine. The inhibitory activity of the resulting NifL mutants towards the NifA protein was assessed using a two-plasmid system in *Escherichia coli*. This consists of a reporter plasmid carrying a *nifH-lacZ* fusion and a second plasmid from which *nifL* and *nifA* are constitutively coexpressed (Söderbäck *et al.*, 1998; Reyes-Ramirez *et al.*, 2002). In *E. coli*, the fixed nitrogen signal is conveyed through the interaction of the C-terminal GHKL domain of NifL with the PII signal transduction proteins (Little *et al.*, 2000; Reyes-Ramirez *et al.*, 2001). Control experiments demonstrated that the reporter fusion was inactive in the absence of NifA and when present, NifA was constitutively active in the absence of NifL (Fig. 1B, bars marked 'Reporter Only' and 'NifA' respectively). When wild-type NifL is present, NifA is only activated when oxygen and fixed nitrogen are limiting (Fig. 1B, black bars). NifA is inhibited by NifL when either oxygen (open bars), excess fixed nitrogen (stripped bars), or both (grey bars) are present. Hence NifL is competent to inhibit NifA in the oxidized state irrespective of the presence of excess fixed-nitrogen. In contrast, alanine substitution in residues lining the FAD cavity produced NifL variants defective in the inhibition of NifA under oxidizing conditions (Fig. 1B compare solid black and open bars). The E70A variant was only partially defective in repressing NifA activity under oxidizing conditions, which is surprising given that E70 is located directly above the N5 position of the FAD and is poised to accept a hydrogen bond from the protonated N5 atom (Key *et al.*, 2007). With the exception of N102A, the mutant proteins remained competent to inhibit NifA in the presence of excess fixed nitrogen (Fig. 1B, stripped and grey bars). The differences in phenotype displayed by the variants are unlikely to represent changes in protein stability, since Western blotting indicated, for example, that N102A was stable under oxidizing conditions, irrespective of the nitrogen source (data not shown). This suggests an important role for the hydrogen-bonding network in transmission of the oxidized-state signal. Replacement of N102, Y110 or H133 with more conservative substitutions also produced variants with a redox signalling phenotype suggesting a requirement for their specific side-chains to maintain the hydrogen-bonding network. However, E70 could be replaced with cysteine or glutamine and retained wild-type function, suggesting that these substitutions can fulfil the redox functions required at this position (Fig. S1).

In order to dismiss the possibility that the redox phenotype of the cavity variants was the consequence of a reduced capacity of NifL to incorporate the FAD prosthetic group, we overexpressed and purified the wild-type PAS1 domain (consisting of residues 1–140) and its variants by nickel affinity chromatography. Wild-type NifL<sub>(1–140)</sub> showed the expected spectral characteristics in the 300–850 nm

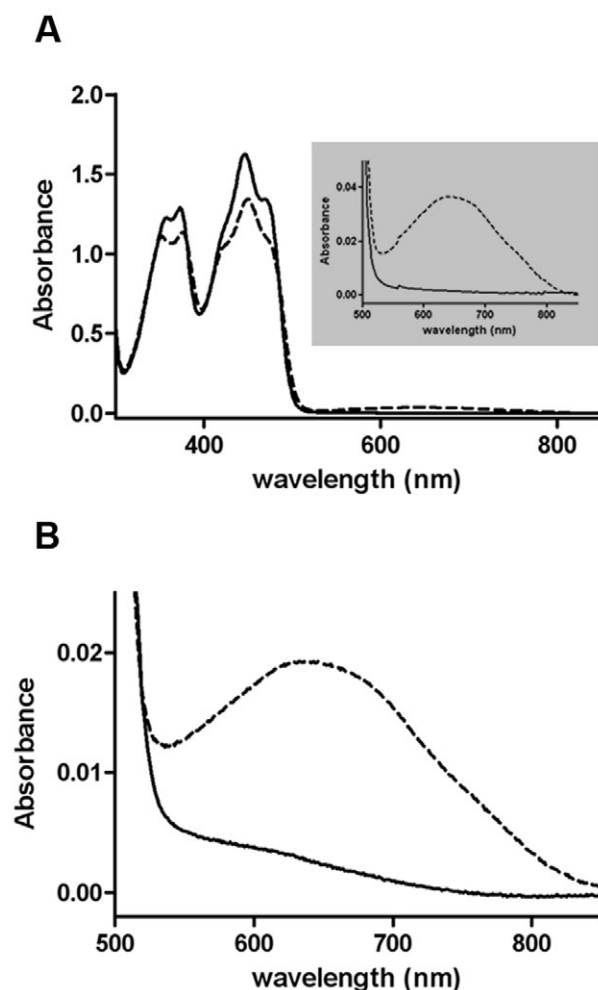


**Fig. 2.** Spectroscopic properties of purified wild-type and E70A-containing PAS1 fragments of NifL at pH 8.0. Spectrophotometry was performed on a Perkin Elmer Lambda 35 UV/VIS spectrophotometer using a 1 cm sample path length and a scan rate of 240 nm min<sup>-1</sup>. A. Visible absorption spectra of the wild-type PAS1 domain (NifL<sub>(1–140)</sub>, solid line) and NifL<sub>(1–140)</sub>-E70A (dashed line). The inset panel shows an expansion of the 500–850 nm spectral region. B. Visible absorption spectrum of NifL<sub>(1–140)</sub>-E70A (dashed line) and of the liberated FAD group following denaturation of NifL<sub>(1–140)</sub>-E70A by addition of solid guanidinium hydrochloride (6 M final concentration) to sample and reference cuvettes (solid line).

region and incorporated 0.7 molecules FAD per monomer, as observed previously for full-length NifL (Hill *et al.*, 1996). Similar values were observed with NifL<sub>(1–140)</sub>-E70Q and NifL<sub>(1–140)</sub>-H133A (data not shown). Notably however, the E70A variant exhibited altered spectral characteristics with a broad absorption band above 550 nm, which is maximal at 640 nm (Fig. 2A). This conferred a green colouration in contrast to the yellow colour of the wild-type, indicative of a charge-transfer complex being formed between the FAD and a ligand (Matthews *et al.*, 1975; Williamson *et al.*, 1982). In order to determine whether the altered spectral

characteristics of NifL<sub>(1–140)</sub>-E70A involved modification of the FAD group, the protein was denatured in 6 M guanidinium hydrochloride to release free flavin. This exhibited a broader absorption centred on 445 nm lacking the pronounced shoulders at 420 and 470 nm conferred by the protein environment, suggesting that FAD had been liberated from the domain, congruent with non-covalent accommodation within the PAS fold. Notably, denaturation with guanidinium hydrochloride was sufficient to abolish the long wavelength charge-transfer absorbance (Fig. 2B). As the free flavin extracted from the E70A variant had identical spectral features to those of wild-type NifL<sub>(1–140)</sub>, it is extremely unlikely that the altered absorption spectrum and the consequent green coloration of the E70A variant arises from FAD modification. Unlike the E70A variant, NifL<sub>(1–140)</sub>-E70Q did not display a green colouration or charge-transfer band in the visible spectrum, as might be predicted from the wild-type phenotype of this substitution (data not shown).

*Involvement of the structurally conserved  $\beta$ -sheet dimer interface in redox signal transmission and oligomerization state*

With the exception of E70, the amino acid residues that line the FAD-binding cavity and contribute to the hydrogen-bonding network linking the isoalloxazine ring to the protein scaffold are all found within the  $\beta$ -sheet backbone of PAS1. This implicates the  $\beta$ -sheet in redox signal transmission. Residues in the  $\beta$ -sheet alternate between those whose side-chains are on the inner surface facing the FAD cofactor and those whose side-chains are on the backside of the cavity and make contacts with flanking  $\alpha$ -helices. A recent study has revealed a highly conserved set of residues located throughout the  $\beta$ -sheet that form an intradimer interface in PAS domains, irrespective of differences in their quaternary structure (Ayers and Moffat, 2008). In *A. vinelandii* NifL, these residues correspond to I40, Y49, V119, L130 and M132 and have side-chains on the outer surface of the  $\beta$ -sheet that mostly pack against the amphipathic A' $\alpha$  helix (N-cap) of the opposing subunit, contributing interactions that result in a tightly packed hydrophobic core between monomers (Fig. 3A).

Given the conserved nature of these residues and their position within a structurally conserved region of the PAS1 domain that may be responsive to the oxidation state of the FAD, we were interested to investigate their potential involvement in redox signal transmission. The conserved  $\beta$ -sheet residues were substituted with alanine and the inhibitory activity of the resulting NifL variants was assessed *in vivo* as described above. Two of the NifL variants, I40A and Y49A, had a 'null' phenotype and were not competent to influence NifA activity under any of four

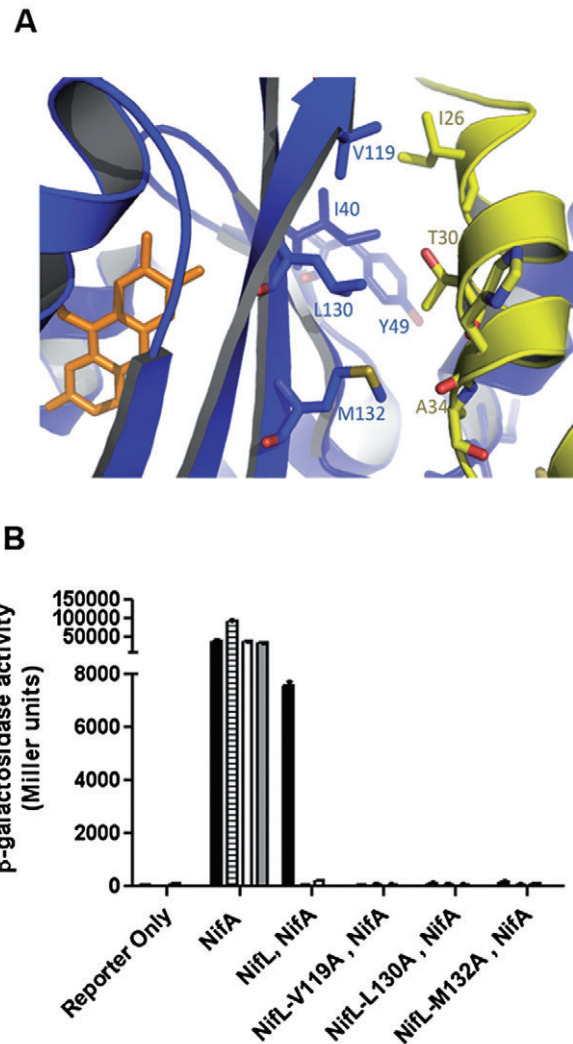


**Fig. 3.** Properties of variant NifL proteins with substitutions in the PAS1  $\beta$ -sheet.

A. The five highly conserved  $\beta$ -sheet residues that face outward from the flavin cavity are labelled in blue and mostly pack against the N-terminal A' $\alpha$  helix (Ncap) of the opposing monomer (yellow) (Key *et al.*, 2007). The isoalloxazine ring of the FAD is shown in orange.

B. Influence of  $\beta$ -sheet substitutions on redox regulation of NifA activity by NifL *in vivo*. Cultures were grown under the following conditions; anaerobically under nitrogen-limiting conditions with casein hydrolysate as the sole nitrogen source (black bars), anaerobically with  $(\text{NH}_4)_2\text{SO}_4$  as nitrogen source (horizontally striped bars), aerobically with casein hydrolysate as the sole nitrogen source (white bars) and aerobically with  $(\text{NH}_4)_2\text{SO}_4$  as nitrogen source (grey bars). All experiments were performed at least in duplicate with error bars denoting the standard error of the mean.

conditions measured. Western blotting analysis suggested that these variants were less stable than wild-type NifL (data not shown), which may account for their inability to inhibit transcriptional activation by NifA. The three remaining variants, V119A, L130A and M132A, exhibited

comparable stability to wild-type NifL; interestingly these stable substitutions inhibited NifA activity under all conditions (Fig. 3B). This behaviour represents the signal 'on' state of NifL and the substitutions apparently lock the protein in an inhibitory conformation that functions as a constitutive anti-activator of NifA. This 'locked-on' phenotype suggests that substitutions replacing conserved residues in the  $\beta$ -sheet of PAS1 trap NifL in an inhibitory form that interacts with NifA irrespective of environmental signals. Since these substitutions are predicted to perturb the subunit interface, we were interested to ascertain if there was any measurable difference in the ability of the variant PAS monomers to associate relative to wild-type PAS1. To pursue this further, we prepared mutant and wild-type PAS1 fusion constructs to permit bacterial two-hybrid analysis (BACTH) (Karimova *et al.*, 1998). Two of the variants (L130A and M132A) retained substantial ability to self-associate relative to the wild-type construct (Fig. 4A). Although the V119A variant failed to exhibit a measurable interaction, Western analysis suggested that one of the hybrid proteins derived from this variant was unstable (Fig. 4B). The lack of an interaction in this case may therefore reflect stability issues with the hybrid proteins under the conditions of the assay.

To further characterize these substitutions, the PAS1 domains of V119A, L130A and M132A were overexpressed as hexahistidine-tagged derivatives of NifL<sub>(1-140)</sub> and their purification attempted. The instability of V119A in the BACTH experiment was mirrored *in vitro* in that the protein leached FAD into the wash fractions during purification and purified as a colourless protein with an FAD content of 0.25 mol per monomer. In contrast, NifL<sub>(1-40)</sub>-L130A and NifL<sub>(1-140)</sub>-M132A were more tractable to purification and yielded fractions with FAD contents of 0.8 and 1.0 mol of FAD per monomer respectively. In both cases, reduction of the FAD moiety occurred at similar rates to wild-type NifL<sub>(1-140)</sub> when the proteins were titrated with sodium dithionite, suggesting that the substitutions do not perturb the redox environment of the FAD group (Fig. S2). Size-exclusion chromatography (SEC) of these PAS1 substitutions was performed to investigate their association state. Previous analysis of the oligomeric state of the wild-type PAS1 domain suggests it elutes as a tetramer on gel filtration (Hefti *et al.*, 2001). In our hands, wild-type NifL<sub>(1-140)</sub> eluted as 5.2 monomer equivalents when SEC was performed at high initial protein concentration (425  $\mu$ M monomer) and as 4.6 monomer equivalents at a lower protein concentration (106  $\mu$ M) (Table 1). The unstable NifL<sub>(1-140)</sub>-V119A variant eluted with the void volume as an aggregated species, but notably the L130A and M132A forms, exhibited more pronounced concentration dependent behaviour, eluting as trimers and tetramers respectively when loaded at high concentration, but

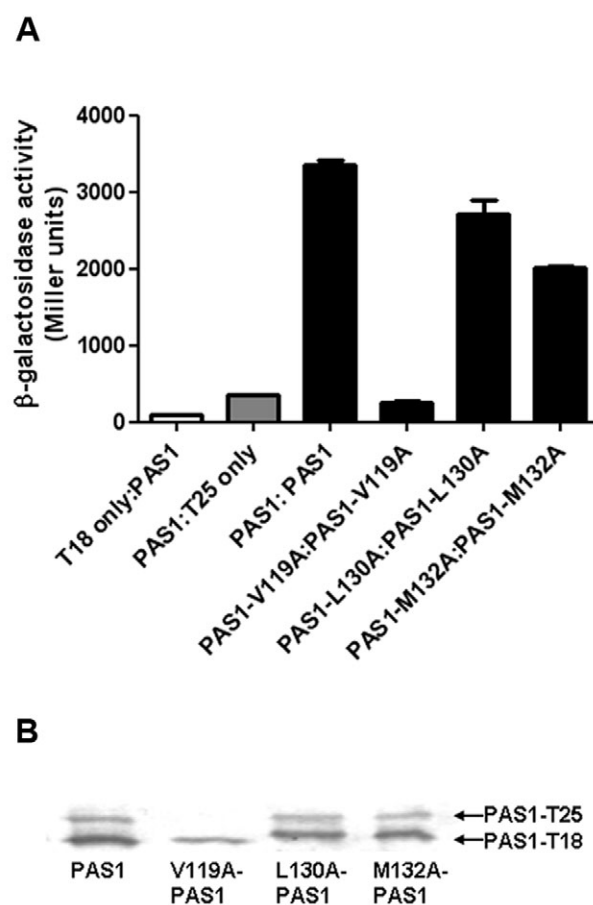


**Fig. 4.** BACTH analysis of oligomerization by  $\beta$ -sheet variants. **A.** Hybrid proteins containing the T18 or T25 subunit of adenylate cyclase from *Bordetella pertussis* fused to the NifL PAS1 domain (NifL residues 1–146) or its mutant variants were constructed and expressed as described in *Experimental procedures*. Black bars represent interactions between two-hybrid proteins while the grey and white bars are controls in which the T18-PAS1 fusion protein is expressed with the T25 subunit only (grey bar) or the T25-PAS1 fusion protein is expressed with the T18 subunit only (white bar). The experiment was performed in duplicate with error bars denoting the standard error of the mean. **B.** Western analysis of the wild-type and mutant hybrid proteins in strains grown under the same conditions as used for the BACTH assay. The upper band represents the hybrid protein containing the T25 subunit of adenylate cyclase and the lower band represents the hybrid protein containing the T18 subunit.

approached the dimeric state when loaded at relatively low concentration (Table 1 and Fig. S3).

To verify these observations and obtain a quantitative insight into the affinities of wild-type and variant PAS1 domains with respect to oligomerization, equilibrium analytical ultracentrifugation (AUC) was undertaken. Fitting the sedimentation equilibrium profiles of wild-type PAS1 to a single component gave a molecular weight corresponding to a multimeric complex containing 3.6–3.7 PAS1 monomers at concentrations between 100 and 10  $\mu$ M (Fig. 5). By fitting the two concentrations to a

**Table 1.** Oligomerization state and FAD content of  $\beta$ -sheet variants of NifL<sub>(1–140)</sub>.

Expression construct <sup>a</sup>	Molecules FAD per monomer	Expected Mw (kDa)	Apparent Mw (kDa) <sup>b</sup>		Apparent oligomeric state	
			425 $\mu$ M	106 $\mu$ M	425 $\mu$ M	106 $\mu$ M
pRL120 (wild-type)	0.7	18.81	96.97	97.33	5.2	4.6
pRL216 (V119A)	0.3	18.78	Void	Void	Aggregated	Aggregated
pRL217 (L130A)	0.8	18.77	54.03	40.00	2.9	2.1
pRL218 (M132A)	1.0	18.75	70.40	46.32	3.8	2.5

a. The histidine tag in the vector pETNdeM-11 provides 26 additional residues at the N-terminus.

b. Derived from the SEC data shown in Fig. S3.

tetramer:dimer reversible equilibrium model using the theoretical molecular weight of dimeric PAS1 a dissociation constant of 0.15  $\mu$ M was obtained. This supports the notion that wild-type PAS1 has a strong tendency to form a tetrameric species. In contrast, fitting the sedimentation equilibrium profiles of NifL<sub>(1–140)</sub>-L130A to a dimer:tetramer model derived a  $K_D$  of 25  $\mu$ M, greater than 100-fold higher than the  $K_D$  relative to the wild-type protein. Congruent with this, fitting NifL<sub>(1–140)</sub>-L130A to a single component species model gave a molecular weight corresponding to 3.0 monomer equivalents at a concentration of 100  $\mu$ M (Fig. 5A) but at a protein concentration of 10  $\mu$ M the molecular weight shifted to 2.3 monomer equivalents (Fig. 5B). Overall, the AUC data substantiate the results from the SEC experiments in demonstrating that wild-type PAS1 is tetrameric in solution (possibly representing a dimer of dimers) and that the L130A substitution drives the equilibrium towards the dimeric state. However, the physiological relevance of the tetrameric association state of the isolated PAS1 domain is not obvious. Given that the L130A substitution is locked in a form that signals the 'on' state it is conceivable that the oxidation state of the FAD influences the dimer-tetramer equilibrium. However, three independent AUC experiments to compare the equilibrium behaviour of the reduced and oxidized forms of the wild-type PAS1 domain at low protein concentration (12  $\mu$ M) failed to reveal any change in association state (data not shown). Given the relatively low dissociation constant for the dimer-tetramer equilibrium in wild-type PAS1, it seems unlikely that the redox signal is conveyed by a major change in association state.

#### *Involvement of the 'N-cap' alpha helix in signalling the oxidized 'on' state*

The crystal structure of oxidized NifL PAS1 reveals that, in common with some other PAS domains, the dimer is stabilized by an N-terminal amphipathic helix that extends from the core PAS fold and is denoted in PAS domains as the A' $\alpha$  helix or the 'N-cap' (Miyatake *et al.*, 2000; Key *et al.*, 2007; Ma *et al.*, 2008). These A' $\alpha$  helices (spanning residues 23–34 of NifL) interact in the PAS1 dimer via

hydrophobic interactions that form a leucine zipper-like structure (Fig. 6A). In addition as noted above, these helices also pack against the hydrophobic surface of the  $\beta$ -sheet of the opposing monomer (Key *et al.*, 2007).

To test the importance of the A' $\alpha$  helix of PAS1 in redox signalling, residues L23–V31 were subjected to alanine scanning and the ability of the resultant NifL mutants to influence NifA transcriptional activity was assessed. Although residue L22 does not form part of the A' $\alpha$  helix it was also included in this analysis as it interacts with the beta sheet residue Y128 in the opposing monomer. Substitutions in residues L22, P24, I26 and F27 that contribute directly to the dimer interface resulted in defects in the ability of NifL to inhibit NifA in response to oxygen (Fig. 6B). However, side-chain specificity is apparently not required at some of these positions as redox signal transmission could be partially or wholly restored by introducing residues other than alanine at positions L22 and I26 (Fig. S4A). Five other alanine substitutions in the A' $\alpha$  helix retained a wild-type phenotype (Fig. S4B). Three of these replaced E25, Q29 or T30, which are located on the hydrophilic face of the helix, whereas V31 makes a reactively minor contribution to the interface. Although R28 is involved in the interaction between the helices, only the hydrophobic portion of its side-chain is required to pack against F27 of the opposing monomer (Fig. 6A). The interactions between L22 and I26 with Y128 of the opposing subunit suggest that Y128 may play a role in signal transmission. Indeed, an alanine substitution in this residue resulted in a redox signalling defective phenotype as the Y128A variant was unable to inhibit NifA activity under oxidizing conditions (Fig. 6B).

Overexpression and purification of the L22Y, I26A and F27A variants as derivatives of NifL<sub>(1–140)</sub> revealed that they exhibited the expected spectral features of oxidized NifL and were replete for FAD. Size-exclusion chromatography of these variants indicated that their oligomerization state is similar to that of the wild-type PAS1 domain (Table S1). This was consistent with bacterial two-hybrid analysis, which revealed no apparent defects in self-association *in vivo*. Furthermore, a PAS fusion protein containing both the L22Y and I26A substitutions gave

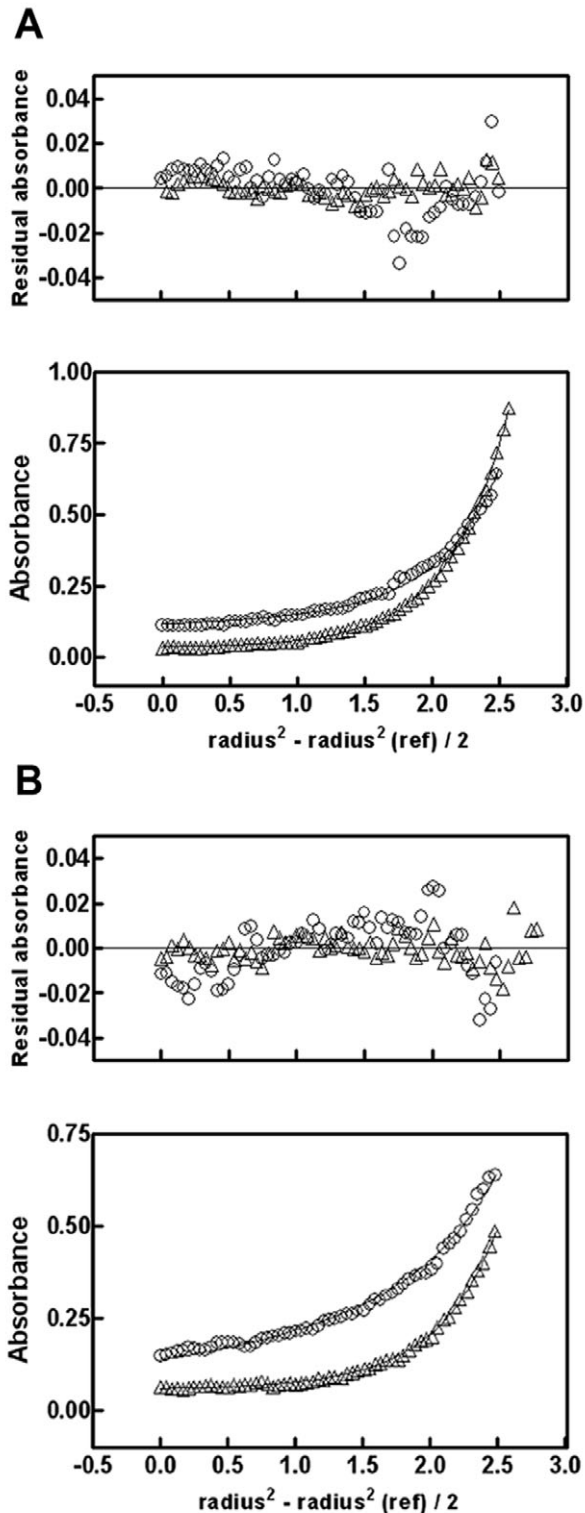


**Fig. 5.** Averaged sedimentation equilibrium profiles of wild-type PAS1 (triangles) and L130A PAS1 (circles) from three independent acquisitions at a rotor speed of 23 000 r.p.m.

Lower panels: (A) Measurements at 460 nm at a protein concentration of 100 μM, (B) measurements at 270 nm at a protein concentration of 10 μM. The lines represent a fit to both data sets for each sample.

Upper panels: residual absorbance between the experimental data and the fitted lines.

domain, the leucine-zipper like interface formed by the N-terminal A'α helices has an important role in effective propagation of the redox signal.

#### *Substitutions in the conserved β-sheet and N-cap regions of PAS1 induce distinct conformational states*

Our results suggest that transmission of the 'on' state redox signal from PAS1 to downstream regions of NifL can be prevented by either disruption of the hydrogen-bonding network surrounding the isoalloxazine moiety of FAD or by substitution of residues that constitute the N-cap dimerization interface of the domain. In contrast, substitution of conserved β-sheet residues results in failure to transmit the 'off' state redox signal. We reasoned that conformational differences corresponding to constitutive 'on' or 'off' signalling states of PAS1 would display differing sensitivities to proteolytic digestion. We have previously observed changes in the pattern of chymotrypsin proteolysis when comparing oxidized and reduced forms of NifL<sub>(1-284)</sub>, a protein fragment containing both the PAS1 and PAS2 domains (Slavny *et al.*, 2010). The major chymotrypsin sensitive sites are primarily located in PAS2 (Money *et al.*, 2001) and the pattern of digestion reflects redox-dependent conformational changes dependent upon the redox state of the FAD cofactor in PAS1 (Slavny *et al.*, 2010). Different mutant classes can therefore be discriminated and subsequently compared with the equivalent wild-type signalling state. Protein samples were incubated with chymotrypsin for various time periods and the progress of proteolysis was monitored by SDS page. As observed previously, the wild-type NifL<sub>(1-284)</sub> fragment digested relatively rapidly under oxidizing conditions, and the band corresponding to the full-length form was completely digested within 10 min (Fig. 7A). An equivalent construct carrying the L130A substitution (NifL<sub>(1-284)</sub>-L130A) digested at a similar rate to that of the wild-type construct under oxidizing conditions. In contrast, the redox signalling variant NifL<sub>(1-284)</sub>-L22Y was highly sensitive to proteolysis and the full-length fragment was digested within 2 min (Fig. 7A). This suggests that NifL<sub>(1-284)</sub>-L130A adopts a similar conformation to that of wild-type NifL<sub>(1-284)</sub> under oxidizing conditions, whereas NifL<sub>(1-284)</sub>-L22Y has a different conformation. To compare the pattern of proteolysis under reducing conditions the

similar activity to the wild-type PAS1 construct in the BACTH assay (Fig. S5). Overall, these results suggest that, although the substitutions examined here do not significantly alter the oligomerization state of the PAS1

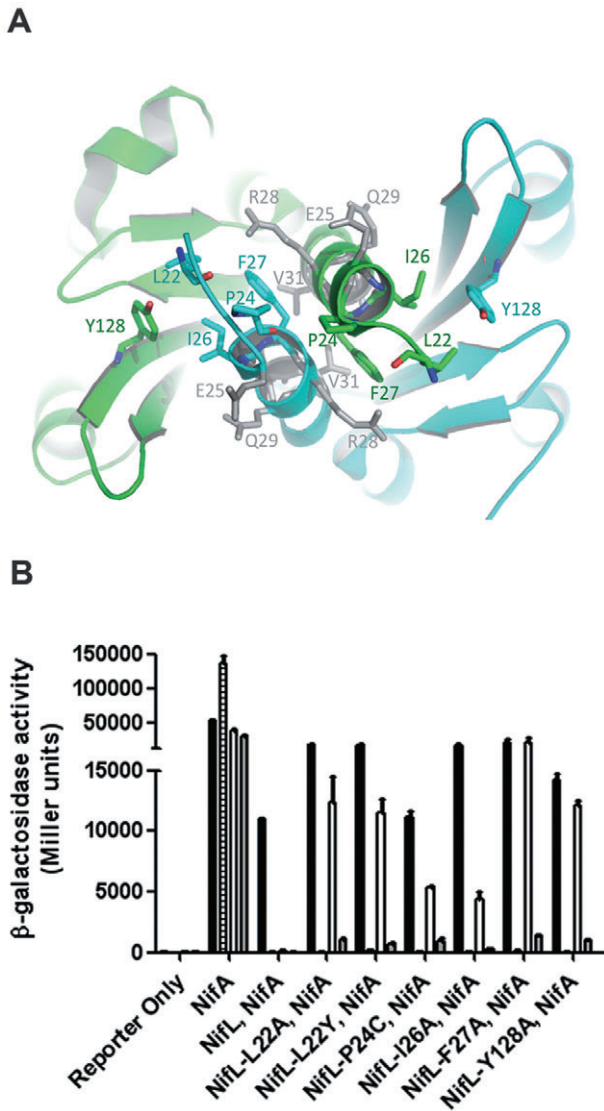


**Fig. 6.** Properties of substitutions in the N-cap region of PAS1. A. The  $\alpha$ -helical dimerization interface of the PAS1 domain (Key *et al.*, 2007), coloured by chain. Residues that give rise to a redox signalling (off) phenotype, when substituted with alanine (or cysteine in the case of P24) are shown in colour. Residues shown in grey give no apparent phenotype when substituted with alanine. B. Influence of substitutions on redox signal transmission *in vivo*. Cultures were grown under the following conditions; anaerobically under nitrogen-limiting conditions with casein hydrolysate as the sole nitrogen source (black bars), anaerobically with  $(\text{NH}_4)_2\text{SO}_4$  as nitrogen source (horizontally striped bars), aerobically with casein hydrolysate as the sole nitrogen source (white bars) and aerobically with  $(\text{NH}_4)_2\text{SO}_4$  as nitrogen source (grey bars). All experiments were performed at least in duplicate with error bars denoting the standard error of the mean.

protocol was repeated following reduction of the FAD cofactor with dithionite. As observed previously, reduced wild-type NifL<sub>(1–284)</sub> exhibited a reduced rate of digestion compared with the oxidized form with a proportion of the full-length fragment remaining undigested after 10 min of

incubation (Fig. 7, compare panels A and B). This difference in the rate of proteolysis suggests a redox-dependent conformational change. In contrast, the NifL<sub>(1–284)</sub>-L130A variant remained sensitive to proteolysis under reducing conditions and digested at a similar rate to that observed under oxidizing conditions. The NifL<sub>(1–284)</sub>-L22Y variant continued to be extremely sensitive to proteolysis under reducing conditions, suggesting that the conformation of this variant is likely to be different to that of NifL<sub>(1–284)</sub>-L130A (Fig. 7). Spectrophotometry of the wild-type and variant proteins confirmed the expected spectral features of NifL FAD under the conditions used for the proteolysis experiments and in all cases the FAD was found to be fully oxidized or fully reduced in the absence or presence of dithionite respectively (data not shown). Taken together, the results suggest that wild-type NifL<sub>(1–284)</sub> exhibits redox-dependent conformational changes that are absent in the two variant proteins. NifL<sub>(1–284)</sub>-L130A appears to be locked in a conformation that resembles the oxidized form of NifL<sub>(1–284)</sub> whereas the L22Y substitution appears to favour a different conformation.

## Discussion

The data presented here suggest a model for redox signal transmission in the PAS1 domain of NifL whereby the redox state of the FAD is communicated via the hydrogen bonding network in the flavin binding cavity to flanking residues in the beta sheet, causing structural changes that are propagated to the dimer interface to influence the arrangement of the N-terminal A' $\alpha$  (N-cap) helices (Fig. 8). This model is supported by the properties of substitutions in discrete structural features that lock the protein either in an 'on' or 'off' signalling state, which according to our limited proteolysis data may resemble the conformation of the oxidized and redox forms of the protein respectively.

Our data support the hypothesis that the hydrogen-bonding network present within the water-filled cavity in the PAS1 structure is important for redox signal transmission (Key *et al.*, 2007). According to this model, protonation of the N5 position of the isoalloxazine ring upon reduction will bring about re-arrangement of hydrogen bonding with the two buried water molecules, leading to transmission of the signal to the  $\beta$ -sheet residues that line the cavity. Non-conservative substitutions in residues S39, N102, Y110 and H133, which are located on the structurally conserved  $\beta$ -sheet and contribute to the network, prevent efficient release of the signal associated with the oxidized status of FAD. Substitution of these residues to alanine results in de-repression of NifA activity under oxidizing conditions as a consequence of NifL remaining in a non-inhibitory conformation that may resemble the reduced form. Thus the conserved  $\beta$ -sheet



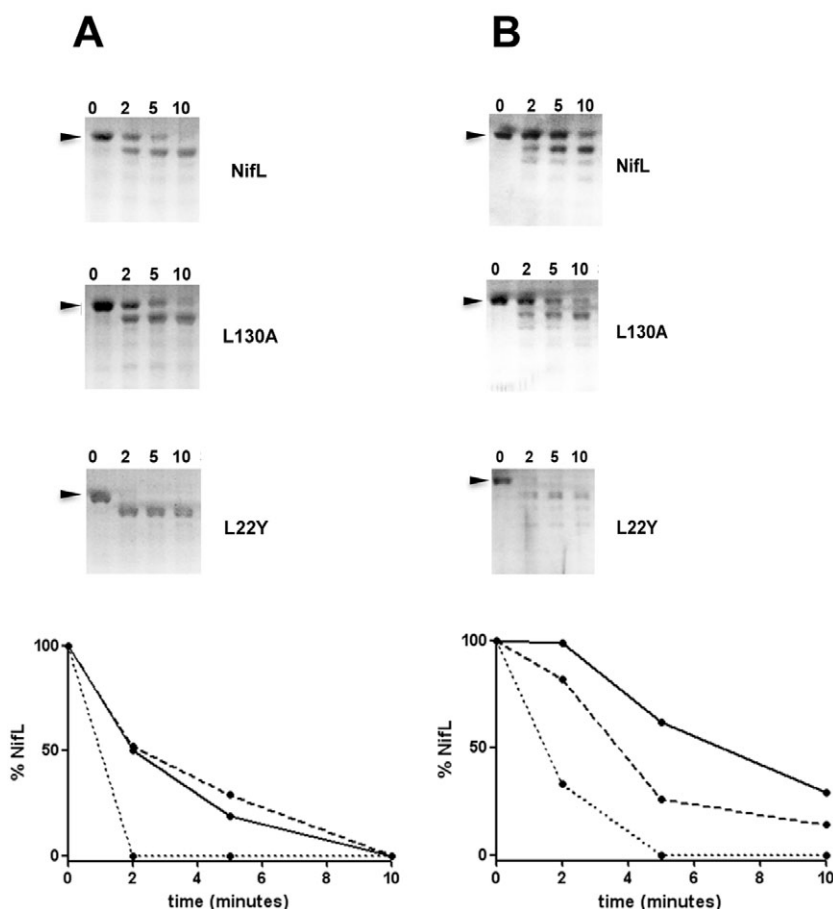


**Fig. 7.** Limited chymotrypsin proteolysis of the PAS1-PAS2 fragment of NifL.

Proteins at a final concentration of 5  $\mu$ M (calculated as a monomer) were incubated with chymotrypsin for 0, 2, 5 and 10 min. Experiments were performed under either oxidizing (A) or reducing (B) conditions. The chymotrypsin: protein ratio was 1:60. Proteolysis was performed on the wild-type PAS1-PAS2 fragment and mutant fragments containing the 'locked-on' substitution L130A or the 'redox signalling' substitution L22Y. In each panel electrophoresis of the PAS1-PAS2 fragment at each time point is represented above a graph plotting the densitometry values obtained for the full-length protein band (marked by the arrowheads). The solid line represents NifL<sub>(1-284)</sub>; dashed line, NifL-L130A<sub>(1-284)</sub>; and dotted line, NifL-L22Y<sub>(1-284)</sub>.

is implicated in transmission of the redox signal from the core of the domain containing the FAD co-factor. Interestingly, E70 located on the E $\alpha$  helix revealed a less distinct redox phenotype upon substitution. Replacement of E70 with alanine reduces the efficacy of the redox response but does not abolish it, whereas the E70C and E70Q substitutions retain a wild-type phenotype. Although E70 forms a hydrogen bond with the side-chain of S39, the relative insensitivity of E70 to substitution suggests that this residue may not occupy a critical position in the signalling pathway, for example, by accepting a proton from the N5 atom of the FAD. However, it has been suggested that the positioning of E70 above the isoalloxazine ring may facilitate formation of the hydroperoxy intermediate formed following attack by dioxygen at the C4 $\alpha$  atom of the reduced FAD. Conceivably, replacement of E70 with alanine may reduce the kinetic efficiency of oxidation and hence lead to a partial redox phenotype. Notably, we observe that the E70A substitution alters the spectral properties of the flavin imparting a green colour characteristic of a charge transfer absorption. Similar long wavelength charge transfer interactions have been observed with a number of oxidized flavoenzymes and low-molecular-weight ligands (Matthews *et al.*, 1975; William-

son *et al.*, 1982). Potentially, the absence of the glutamate side-chain may either influence the proximity of another protein ligand to the FAD or, alternatively, stabilize the interaction with an oxidized intermediate, thus promoting the charge-transfer interaction. Intriguingly, altered FAD spectral properties are also observed in the PAS domain of *Acetobacter xylinum* AxDGC2, when a histidine residue that is predicted to stack above the isoalloxazine ring in a similar position to NifL E70, is substituted with alanine (Qi *et al.*, 2009). As in the case of NifL PAS1, the His to Ala substitution in AxDGC2 does not completely block redox signal transmission. However, in this example, the substitution promotes covalent modification of the FAD, probably as a consequence of attack by oxygen on the C6 atom to form 6-hydroxy-FAD (Qi *et al.*, 2009).

We sought to investigate the effect of substituting  $\beta$ -sheet residues with side-chains orientated away from the FAD binding cavity. A previous study of PAS quaternary structures has identified a set of five  $\beta$ -strand residues that are conserved in the dimer interface of diverse PAS structures (Ayers and Moffat, 2008). Although stability issues prevented detailed examination of two of these core residues, alanine replacements of V119, L130 and M132 resulted in constitutive inhibition of NifA activity and

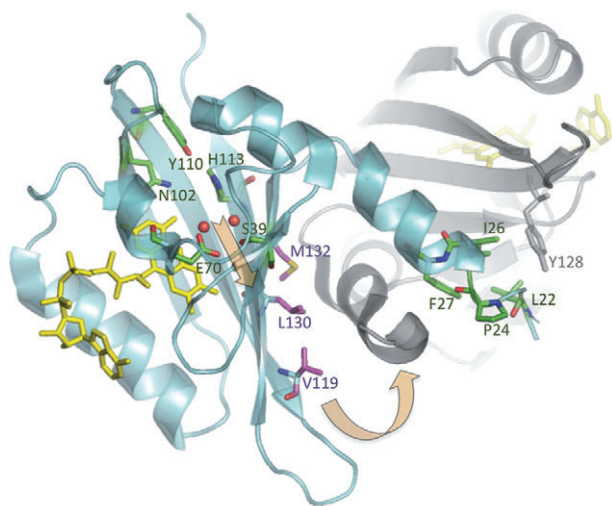


**Fig. 8.** Proposed redox signal transmission pathway for the PAS1 domain. For simplicity only specific side-chains in chain B (cyan) are highlighted, with the exception of Y128 in chain A (grey). The internal water molecules in the FAD cavity are depicted as red spheres and the FAD is shown in yellow. Substitutions of residues (shown as stick models) with C atoms coloured in green lead to a redox signalling 'off' phenotype, whereas alanine substitutions in residues with C atoms coloured in purple result in a locked 'on' phenotype. Signal perception within the flavin cavity is proposed to induce a conformational change in the  $\beta$ -sheet, which is propagated towards the N-cap helix of the opposing monomer (indicated by the orange arrows).

hence apparently lock PAS1 in the 'on' state. Since the redox properties of the FAD are apparently unaltered by the alanine substitutions, these highly conserved hydrophobic residues appear to play a key role in redox signal transmission. However, despite the importance of these residues for subunit interactions, alanine substitutions of L130 and M132 do not completely disrupt the dimer interface, but shift the tetramer–dimer equilibrium of PAS1 towards the dimeric state. The physiological function of tetramer formation is not understood, as the tetramer–dimer equilibrium does not appear to be influenced by the redox state of the FAD. Although the first 20 N-terminal amino acids of NifL, which are unresolved in the crystal structure, appear to have a role in PAS1 tetramerization, an N-terminal truncated version of NifL lacking the first 19 residues gives a wild-type level of response to the redox and fixed nitrogen status (R. Little and R. Dixon, unpubl. res.). Since V119, L130 and M132 have their side-chains orientated towards the A' $\alpha$  helix (N cap) of the opposing monomer, it is reasonable to suppose that the N-cap residues will be sensitive to redox dependent changes in the  $\beta$  sheet. This may provide a pathway for transmission of the signal to the PAS surface that may invoke re-arrangement of the quaternary structure as a means of signal propagation (Fig. 8).

Alanine scanning of the A' $\alpha$  helix revealed the importance of four residues in the dimer interface that make

important contributions to redox signalling. In contrast to the aforementioned  $\beta$ -sheet substitutions, these variants result in an 'off' state whereby oxidation of the FAD fails to generate an inhibitory conformer of NifL. Limited proteolysis of one variant, L22Y, indicates that the conformation of the PAS domains is similar to that of the reduced form of NifL, irrespective of the redox state of the FAD. Two of the four residues, P24 and F27, make direct contributions to the  $\alpha$  helical interface, whereas L22 and I26 pack against the N-terminal region of the I $\beta$  strand of the opposing monomer through interactions with Y128. Given the interfacial nature of these residues in the dimer, it is perhaps surprising that none of these variants appeared to influence the oligomerization state of the PAS1 domain, even when the L22Y and I26A substitutions were combined. However, considering the extended nature of the dimer interface, involving both the  $\beta$  sheet and the N-terminal helices, it is possible that the substitutions invoke relatively small changes in quaternary structure that, for example, may reorient the subunits in relationship to each other. Clearly, the integrity of the N-cap interface appears to be critical for effective signal transmission, supporting the model in which redox signal transmission propagates from the  $\beta$ -strands lining the FAD cavity to the N-terminal  $\alpha$  helices.

Taken together, our structure-guided mutagenesis of the PAS1 domain of NifL suggests an inter-subunit pathway for redox signal transmission whereby the redox signal sensed at the core of PAS1 is transmitted to the surface of the domain via the dimer interface. In this model, the conserved  $\beta$ -sheet functions to convert the primary redox signal detected as a change in oxidation state of the FAD to a structural signal in which changes in the packing topography influence specific interactions between the  $\beta$ -sheet and the A' $\alpha$  helix of the opposing monomer. Given the opposing phenotypes of substitutions in the extended dimer interface, it is possible to posit functional roles for specific residues in the  $\beta$ -strand and A' $\alpha$  helices in switching between the 'on' and 'off' states. Since removal of the side-chains of the  $\beta$ -strand residues V119, L130 and M132 leads to a 'locked on phenotype', it would appear that these residues play an important role in signalling the reduced state of the FAD. Hence, under reducing conditions these residues may engage with the N-terminal  $\alpha$  helix of the opposing monomer, resulting in re-arrangement of the  $\alpha$  helical interface. Conversely, substitutions in residues that maintain the  $\alpha$  helical interface (F27 and P24) or interact with the I $\beta$ -strand (L22 and I26) result in a 'locked off' phenotype and therefore these inter-subunit interactions are important for establishment of the 'on' state signalled by oxidation of the FAD. It is feasible that these interactions are altered when the FAD is reduced leading to a reorganization of the dimer interface and consequent repositioning of the N-cap  $\alpha$  helices

(Fig. 8). A similar pathway of signal transmission has been proposed for the FAD containing PAS domain of the *E. coli* aerotaxis receptor, Aer, whereby re-organization of the hydrogen-bonding network in the flavin binding cavity is proposed to promote structural changes in the  $\beta$ -scaffold that are propagated to the N-cap. In this model the N-cap helix is proposed to pack against the  $\beta$ -scaffold in the 'off' state whereas the 'on' state brings about re-organization of the N-cap such that the PAS core is accessible to the adjacent HAMP domain (Campbell *et al.*, 2010). Residues in the conserved interface in the PAS  $\beta$ -scaffold of Aer have been demonstrated to interact directly with the HAMP domain, which is required for the proper folding of the PAS domain and stable binding of the FAD. A cysteine substitution of one of the highly conserved hydrophobic residues in the I $\beta$ -strand, I114 (equivalent to M132 in NifL) gives rise to a 'signal on' phenotype *in vivo* and forms a disulphide bond with a cysteine residue in the HAMP domain (Campbell *et al.*, 2010). However, the mode of signal transmission in Aer is different to that of NifL, since the PAS monomers in the Aer domain model are not predicted to interact with each other in the dimer (Watts *et al.*, 2008). It therefore seems likely that redox signal transmission in the PAS domain of Aer involves intra-subunit interactions between the N-cap and the PAS core rather than the inter-subunit model proposed for NifL. Analogous intra-subunit interactions between the amphipathic N-cap helix and the  $\beta$ -scaffold are observed in the fungal photoreceptor VVD, but in this case they control the association state of the PAS domain. In the dark state the PAS domain of VVD is monomeric and the N-terminal  $\alpha$  helix packs against the PAS core. Upon light activation, the N-cap is displaced away from the core PAS domain, promoting interaction of the N-cap helices in adjacent subunits to form the light state dimer (Zoltowski *et al.*, 2007; Zoltowski and Crane, 2008).

The NifL protein contains a second PAS domain (PAS2) located downstream of PAS1. We have recently demonstrated a role for this domain in relaying the redox signal from the FAD-containing PAS1 domain to the C-terminal histidine kinase-like effector region of the protein. As is the case for PAS1, the dimer interface in this second PAS domain appears to play a major role in signal transmission. In contrast, to the signal-induced structural re-arrangement in PAS1, which appears to be relatively subtle, transmission of the redox signal to the downstream PAS2 domain influences the monomer–dimer equilibrium to favour dissociation of the PAS2 subunits under oxidizing conditions (Slavny *et al.*, 2010). This may serve to amplify the structural signal, and provide sufficient structural flexibility to promote the conformational movements required to switch the activity of the C-terminal domains of NifL. This mechanism of signal relay in NifL is analogous to the ligand-induced dimeric

switch in the sensory domain of the DctB histidine kinase, which also contains tandem PAS domains (Zhou *et al.*, 2008). Binding of succinate to the membrane distal PAS domain (DctBpd) disrupts the dimer interface, resulting in activation of kinase activity. Substitutions at different locations in the dimerization interface lock DctB in either the 'on' or the 'off' states independent of ligand binding, as a consequence of their influence on the monomer–dimer equilibrium (Nan *et al.*, 2010).

How is the structural signal relayed from PAS1 to PAS2 in the case of NifL? Tandem PAS domains are typically linked by short amphipathic  $\alpha$ -helices (Möglich *et al.*, 2010) and NifL is predicted to contain such an  $\alpha$ -helical region (residues 137–150) between the PAS1 to PAS2 domains. A similar  $\alpha$ -helical linker connects the FAD containing PAS-A domain to the second PAS domain (PAS-B) in the MmoS redox sensor from *Methylococcus capsulatus* (Ukaegbu and Rosenzweig, 2009). In both cases, the redox signal generated by the FAD co-factor in the N-terminal PAS domain could be propagated along this helix to the second PAS domain, via changes in torque or helical rotation, as has been proposed for several well-characterized PAS-containing proteins (Möglich *et al.*, 2009; 2010).

Overall, the picture emerging from the current and previous structure/function analysis of FAD containing PAS domains (Key *et al.*, 2007; Qi *et al.*, 2009; Ukaegbu and Rosenzweig, 2009; Campbell *et al.*, 2010) suggests a common mechanism for redox signal transmission in which redox chemistry at the FAD determines the organization of the water-mediated hydrogen bonding network within the internal cavity, which is relayed to the  $\beta$ -sheet surface and on to the N-terminal  $\alpha$ -helix. The NifL PAS1 domain belongs to a sub-class of PAS containing proteins (e.g. EcDos, SmFixL and H-NOX) in which dimerization is stabilized by interactions between the amphipathic N-cap helices. Our results demonstrate for NifL that the dimer interface between the PAS1 monomers is critical for signal transmission. Signal-induced structural perturbations may influence both interactions between the N-terminal  $\alpha$ -helices themselves and their interface with the  $\beta$ -sheet surface in the opposing monomer. By analogy with the signal-dependent conformational changes observed in other PAS domains that form stable dimers, these quaternary structure perturbations might be relatively small, perhaps involving a scissor-like motion that rotates the subunits with respect to each other (Kurokawa *et al.*, 2004; Möglich and Moffat, 2007; Ayers and Moffat, 2008). However, it is also possible that, rather than promoting changes in the spatial orientation of the subunits, these interactions may drive conformational changes in the dimer that provide signal output. Although, small changes in conformation or quaternary structure may in principle lead to large differences in free energy, the additional

structural output provided by relaying the signal from PAS1 to PAS2 may provide the conformational flexibility required to drive the C-terminal kinase-like domains of NifL into the appropriate conformer.

## Experimental procedures

### Site-directed mutagenesis

All mutants were constructed using a two-step PCR approach. The first step consisted of two independent PCR reactions. One reaction was carried-out with the forward primer pa1 (5'-CTAGAGAATTCGGATAGACGAGGCACC-3') and a reverse primer containing the desired mutation. The second reaction was carried-out with either the reverse primer NifLrev (5'-GCTCGGGTTGGAGAGCATCAC-3') or primer MS2Rev (5'-GCGCGAAGAACACGTGGGCCCTG-3') and a forward primer containing the same desired mutation. The products from the first step PCR reactions were purified (Qiagen PCR purification kit) and used as template DNA for the second step PCR reaction using the primer pa1 and either NifLrev or MS2Rev (see above). The resulting fragment was purified (Qiagen PCR purification kit) and digested with the restriction endonuclease enzymes, NdeI and MluI (Roche). The digested fragment was cloned into the pT7-7-derived vector, pPR34 containing the co-transcribed *nifL* and *nifA* genes (Söderbäck *et al.*, 1998). The presence of all mutations was confirmed by DNA sequencing.

### $\beta$ -Galactosidase assays

Growth conditions and  $\beta$ -galactosidase assays to determine NifA transcriptional activity were performed as described previously (Perry *et al.*, 2005; Little *et al.*, 2007).  $\beta$ -Galactosidase assays for BACTH analysis were carried-out according to the same procedure with the exception that all cultures were grown anaerobically in sealed plastic vials (internal volume 7 ml) at 30°C in Luria–Bertani (LB) medium supplemented with 1% glucose, 0.5 mM IPTG (isopropyl- $\beta$ -D-thiogalactopyranoside) and appropriate antibiotics.

### Plasmid construction for protein overexpression and protein purification

Plasmids pRL90, pRL91, pRL92, pRL94 and pRL97 encoding L22Y, I26A, F27A, E70A and wild-type NifL PAS1<sub>(1–140)</sub> in pET28a(+) respectively were prepared by PCR using the corresponding pPR34-based vectors (see above) as template. PCR with the forward primer pa1 (see above) and the reverse primer L140StopBam (5'-CGAAGGATCCTCA GTGCAATTCGCTGGTGTGCGC-3') produced a DNA fragment encoding the appropriate NifL residues and desired mutation flanked by a 5' NdeI site and a 3' BamHI site. The PCR products were purified (Qiagen PCR purification kit) and digested with the restriction endonucleases NdeI and BamHI and cloned into plasmid pET28a(+).

Plasmids pRL120, pRL217 and pRL218 encoding wild-type, L130A and M132A NifL PAS1<sub>(1–140)</sub>, respectively, were prepared by PCR in the same way as above but were cloned

into a plasmid derived from pETM-11 (named pETNdeM-11) in which the NcoI site in the multiple cloning region is mutated to yield an NdeI site.

Plasmids pRL121, pRL221 and pRL336 encoding wild-type NifL<sub>(1–284)</sub>, NifL<sub>(1–284)</sub>-L130A and NifL<sub>(1–284)</sub>-L22Y in pETNdeM-11, respectively, were prepared by PCR using the corresponding pPR34-based vectors as template. PCR with the forward primer pa1 (5'-CTAGAGAATTCGGATAGACGAGGCACC-3') and the reverse primer L284StopBam (5'-CGAAGGATCCT CACTTCAGCGCGTTGAGCCGC-3') produced a DNA fragment encoding the appropriate NifL residues and desired mutation flanked by a 5' NdeI site and a 3' BamHI site. The PCR products were purified (Qiagen PCR purification kit) and digested with the restriction endonucleases NdeI and BamHI and cloned into plasmid pETNdeM-11. All constructs were confirmed by DNA sequencing.

In all cases overexpression was carried-out in *E. coli* BL21(DE3)pLysS cells. Cultures were grown aerobically in LB medium and expression from the T7 promoter was induced by the addition of IPTG to a final concentration of 1 mM. Proteins were purified as described previously (Little and Dixon, 2003; Little *et al.*, 2007; Slavny *et al.*, 2010)

### BACTH analysis

Plasmids pPS93, pRL131, pRL132, pRL159, pRL257, pRL258 and pRL256 encode wild-type, L22Y, I26A and L22Y/I26A, V119A, L130A and M132A NifL PAS1<sub>(1–146)</sub> respectively in BACTH vector pUT18. Plasmids pPS98, pRL134, pRL135, pRL160, pRL259, pRL160 and pRL261 encode wild-type, L22Y, I26A and L22Y/I26A, V119A, L130A and M132A NifL PAS1<sub>(1–146)</sub>, respectively, in BACTH vector pT25. To construct the vectors, a DNA fragment encoding the protein fragment of interest flanked by a 5' BamHI site and a 3' KpnI site were generated by PCR. The forward primer NifL-BTH-F (5'-GAGGATCCCATGACCCCGGCCAACCCGAC-3') and PAS1-BTH-1R (5'-CTTAGGTACCACGCGTTGTTCCAG-3') were used to amplify the region of *nifL* encoding amino acids 1–146. Plasmid pPR34 or derivative plasmids containing the desired mutation were used as template DNA. PCR products were purified (Qiagen PCR purification kit), digested with the restriction endonucleases KpnI and BamHI and cloned into the BACTH vectors pT25 (Karimova *et al.*, 1998) and pUT18 (Euromedex). All constructs were confirmed by DNA sequencing and were co-transformed into chemically competent BTH101 cells (*F'*, *cya*-99, *ara*D139, *gal*E15, *gal*K16, *rps*L1 [Str<sup>R</sup>], *hsd*R2, *mcr*A1, *mcr*B1) (Karimova *et al.*, 1998) and plated onto LB medium supplemented with Xgal (40  $\mu$ g ml<sup>-1</sup>), chloramphenicol (30  $\mu$ g ml<sup>-1</sup>), carbenicillin (100  $\mu$ g ml<sup>-1</sup>) and IPTG (0.5 mM). Agar plates were incubated at 30°C for 72 h and colonies were checked for homogeneity before being assayed for  $\beta$ -galactosidase activity as described above.

### Western blotting

To obtain protein extracts, cultures of ET8000 or BTH101 cells containing the plasmid(s) of interest were grown as for the  $\beta$ -galactosidase assays. To ensure that cell numbers were equivalent between samples, the volume taken from

each culture was adjusted according to differences in OD<sub>600</sub>. The normalized cell samples were centrifuged and the pellet re-suspended in protein loading buffer (125 mM Tris-Cl, 4% sodium dodecyl sulphate, 20% glycerol, 10% β-mercaptoethanol, 0.05% bromophenyl blue, pH 6.8). The proteins were separated by SDS-PAGE and electrotransferred onto nitrocellulose membranes. Membranes were probed with polyclonal antisera against NifL and primary antibodies were detected with alkaline-phosphatase-conjugated anti-rabbit secondary antibodies. Secondary antibodies were detected by staining with 5-bromo-4-chloro-3-indolylphosphate and nitroblue tetrazolium.

#### Size-exclusion chromatography

Size-exclusion chromatography was performed over a Superose 12 10/300 GI column (G E Healthcare) at a flow rate of 0.5 ml min<sup>-1</sup>. Chromatography of NifL PAS<sub>1(1-140)</sub> mutants V119A, L130A and M132A was performed in 50 mM Tris-Cl, 10% glycerol, 200 mM NaCl, pH 7.5. Chromatography of NifL PAS<sub>1(1-140)</sub> mutants L22Y, I26A and F27A was performed in 50 mM Tris-Cl, 15% glycerol, 200 mM NaCl, 20 mM imidazole, pH 7.5. Bio-Rad gel filtration standards (thyroglobulin [bovine], γ-globulin [bovine], ovalbumin [chicken], myoglobin [horse] and vitamin B12) were used for calibration.

#### Analytical ultracentrifugation

Sedimentation equilibrium experiments were performed in a Beckman Optima XL analytical ultracentrifuge equipped with absorbance optics and an An50-Ti rotor. The NifL PAS<sub>1(1-140)</sub> domain was diluted to concentrations of 10 and 100 μM (determined spectroscopically and calculated as a monomer). Proteins were prepared in a final buffer composition of 50 mM KH<sub>2</sub>PO<sub>4</sub> (pH 8.0), 100 mM NaCl. Each sample (120 μl) was loaded into the sample sector of a charcoal-filled Epon double sector cell fitted with quartz windows, while 120 μl buffer was loaded into the reference sector. Samples were centrifuged at speeds of 19 000 and 23 000 r.p.m. and the absorbance was recorded at 270 nm at a concentration of 10 μM protein and at 460 nm for protein concentrations of 100 μM. The parameters for buffer density and partial specific volume were determined using SEDNTERP. Data analysis was executed using Ultrascan II (Demeler, 2005) where profiles of individual samples were initially analysed at single speeds using an ideal, single-component model. Subsequent analysis of each PAS<sub>1</sub> form used simultaneous fitting of both speed and concentrations to a tetramer–dimer reversible equilibrium model where the theoretical dimer weight was fixed and the tetramer–dimer dissociation constant was fitted.

#### Limited chymotrypsin proteolysis

Chymotrypsin proteolysis was performed in TA buffer (50 mM Tris-acetate, pH 7.0, 100 mM potassium acetate, 8 mM magnesium acetate, 1 mM dithiothreitol) at 27.5°C. NifL<sub>(1-284)</sub> protein fragments were diluted from 50 μM initial dilutions (calculated as monomeric concentrations) to a final concentration of 5 μM in a reaction volume of 120 μl. Digestion of

samples was initiated by the addition of α-chymotrypsin (Sigma Chemical; from bovine pancreas) from a 0.5 mg ml<sup>-1</sup> stock solution to a final chymotrypsin: NifL<sub>(1-284)</sub> weight : weight ratio of 1:60. At the times indicated in Fig. 7, 15 μl of the sample was withdrawn and added to a microcentrifuge tube containing 0.35 μg of chymotrypsin inhibitor (Roche). An equal volume of ×2 SDS-PAGE gel-loading buffer was added and the sample was heated to 100°C for 6 min. SDS-PAGE was performed using 6 μl of sample on 12% pre-cast polyacrylamide gels (Expedeon). For reducing conditions, all samples and reagents were transferred to a Belle anaerobic chamber (in which the oxygen level was maintained below 2.5 p.p.m.). The 50 μM protein pre-dilutions were reduced by the addition of 1 M sodium dithionite to a final concentration of 5 mM. A subsample of each protein was removed from the chamber in a sealed cuvette and reduction of the sample was confirmed by spectrophotometry. Dithionite was added to the final reaction tubes to a final concentration of 5 mM prior to addition of the 50 μM reduced protein solution. The proteolysis experiment was then performed as described above.

#### Acknowledgements

This work was supported by an Institute Strategic Programme Grant from the Biotechnology and Biological Sciences Research Council (BBSRC). Paloma Salinas was supported by a fellowship from the Conselleria d'Empresa, Universitat i Ciència, Generalitat Valenciana, Spain.

#### References

- Ayers, R.A., and Moffat, K. (2008) Changes in quaternary structure in the signaling mechanisms of PAS domains. *Biochemistry* **47**: 12078–12086.
- Campbell, A.J., Watts, K.J., Johnson, M.S., and Taylor, B.L. (2010) Gain-of-function mutations cluster in distinct regions associated with the signalling pathway in the PAS domain of the aerotaxis receptor, Aer. *Mol Microbiol* **77**: 575–586.
- Demeler, B. (2005) UltraScan – a comprehensive data analysis software package for analytical ultracentrifugation experiments. In *Analytical Ultracentrifugation*. Scott, D., Harding, S., and Rowe, A. (eds). Cambridge: RSC Publishing, pp. 210–229.
- Dixon, R., and Kahn, D. (2004) Genetic regulation of biological nitrogen fixation. *Nat Rev Microbiol* **2**: 621–631.
- Hefti, M.H., Van Vugt-Van der Toorn, C.J.G., Dixon, R., and Vervoort, J. (2001) A novel purification method for histidine-tagged proteins containing a thrombin cleavage site. *Anal Biochem* **295**: 180–185.
- Hill, S., Austin, S., Eydmann, T., Jones, T., and Dixon, R. (1996) *Azotobacter vinelandii* NIFL is a flavoprotein that modulates transcriptional activation of nitrogen-fixation genes via a redox-sensitive switch. *Proc Natl Acad Sci USA* **93**: 2143–2148.
- Karimova, G., Pidoux, J., Ullmann, A., and Ladant, D. (1998) A bacterial two-hybrid system based on a reconstituted signal transduction pathway. *Proc Natl Acad Sci USA* **95**: 5752–5756.
- Key, J., Hefti, M., Purcell, E.B., and Moffat, K. (2007) Structure of the redox sensor domain of *Azotobacter vinelandii*

- NifL at atomic resolution: signaling, dimerization, and mechanism. *Biochemistry* **46**: 3614–3623.
- Kurokawa, H., Lee, D.-S., Watanabe, M., Sagami, I., Mikami, B., Raman, C.S., and Shimizu, T. (2004) A redox-controlled molecular switch revealed by the crystal structure of a bacterial heme PAS sensor. *J Biol Chem* **279**: 20186–20193.
- Little, R., and Dixon, R. (2003) The amino-terminal GAF domain of *Azotobacter vinelandii* NifA binds 2-oxoglutarate to resist inhibition by NifL under nitrogen-limiting conditions. *J Biol Chem* **278**: 28711–28718.
- Little, R., Reyes-Ramirez, F., Zhang, Y., van Heeswijk, W.C., and Dixon, R. (2000) Signal transduction to the *Azotobacter vinelandii* NIFL-NIFA regulatory system is influenced directly by interaction with 2-oxoglutarate and the PII regulatory protein. *EMBO J* **19**: 6041–6050.
- Little, R., Martinez-Argudo, I., Perry, S., and Dixon, R. (2007) Role of the H domain of the histidine kinase-like protein NifL in signal transmission. *J Biol Chem* **282**: 13429–13437.
- Ma, X., Sayed, N., Baskaran, P., Beuve, A., and van den Akker, F. (2008) PAS-mediated dimerization of soluble guanylyl cyclase revealed by signal transduction histidine kinase domain crystal structure. *J Biol Chem* **283**: 1167–1178.
- Macheroux, P., Hill, S., Austin, S., Eydmann, T., Jones, T., Kim, S.-O., et al. (1998) Electron donation to the flavoprotein NifL, a redox-sensing transcriptional regulator. *Biochem J* **332**: 413–419.
- Martinez-Argudo, I., Little, R., Shearer, N., Johnson, P., and Dixon, R. (2004) The NifL-NifA system: a multidomain transcriptional regulatory complex that integrates environmental signals. *J Bacteriol* **186**: 601–610.
- Matthews, R.G., Massey, V., and Sweeley, C.C. (1975) Identification of p-hydroxybenzaldehyde as the ligand in the green form of old yellow enzyme. *J Biol Chem* **250**: 9294–9298.
- Miyatake, H., Mukai, M., Park, S.-Y., Adachi, S.-I., Tamura, K., Nakamura, H., et al. (2000) Sensory mechanism of oxygen sensor FixL from *Rhizobium meliloti*: crystallographic, mutagenesis and resonance raman spectroscopic studies. *J Mol Biol* **301**: 415–431.
- Möglich, A., and Moffat, K. (2007) Structural basis for light-dependent signaling in the dimeric LOV domain of the photosensor YtvA. *J Mol Biol* **373**: 112–126.
- Möglich, A., Ayers, R.A., and Moffat, K. (2009) Structure and signaling mechanism of Per-ARNT-Sim domains. *Structure* **17**: 1282–1294.
- Möglich, A., Ayers, R.A., and Moffat, K. (2010) Addition at the molecular level: signal integration in designed Per-ARNT-Sim receptor proteins. *J Mol Biol* **400**: 477–486.
- Money, T., Barrett, J., Dixon, R., and Austin, S. (2001) Protein–protein interactions in the complex between the enhancer binding protein NIFA and the sensor NIFL from *Azotobacter vinelandii*. *J Bacteriol* **183**: 1359–1368.
- Nan, B., Liu, X., Zhou, Y., Liu, J., Zhang, L., Wen, J., et al. (2010) From signal perception to signal transduction: ligand-induced dimeric switch of DctB sensory domain in solution. *Mol Microbiol* **75**: 1484–1494.
- Perry, S., Shearer, N., Little, R., and Dixon, R. (2005) Mutational analysis of the nucleotide-binding domain of the anti-activator NifL. *J Mol Biol* **346**: 935–949.
- Qi, Y., Rao, F., Luo, Z., and Liang, Z.-X. (2009) A flavin cofactor-binding PAS domain regulates c-di-GMP synthesis in AxDGC2 from *Acetobacter xylinum*. *Biochemistry* **48**: 10275–10285.
- Reyes-Ramirez, F., Little, R., and Dixon, R. (2001) Role of *Escherichia coli* nitrogen regulatory genes in the nitrogen response of the *Azotobacter vinelandii* NifL-NifA complex. *J Bacteriol* **183**: 3076–3082.
- Reyes-Ramirez, F., Little, R., and Dixon, R. (2002) Mutant forms of the *Azotobacter vinelandii* transcriptional activator NifA resistant to inhibition by the NifL regulatory protein. *J Bacteriol* **184**: 6777–6785.
- Slavny, P., Little, R., Salinas, P., Clarke, T.A., and Dixon, R. (2010) Quaternary structure changes in a second Per-ARNT-Sim domain mediate intramolecular redox signal relay in the NifL regulatory protein. *Mol Microbiol* **75**: 61–75.
- Söderbäck, E., Reyes-Ramirez, F., Eydmann, T., Austin, S., Hill, S., and Dixon, R. (1998) The redox- and fixed nitrogen-responsive regulatory protein NIFL from *Azotobacter vinelandii* comprises discrete flavin and nucleotide-binding domains. *Mol Microbiol* **28**: 179–192.
- Taylor, B.L., and Zhulin, I.B. (1999) PAS domains: internal sensors of oxygen, redox potential, and light. *Microbiol Mol Biol Rev* **63**: 479–506.
- Ukaegbu, U.E., and Rosenzweig, A.C. (2009) Structure of the redox sensor domain of *Methylococcus capsulatus* (Bath) MmoS. *Biochemistry* **48**: 2207–2215.
- Watts, K.J., Johnson, M.S., and Taylor, B.L. (2008) Structure-function relationships in the HAMP and proximal signaling domains of the aerotaxis receptor Aer. *J Bacteriol* **190**: 2118–2127.
- Williamson, G., Engel, P.C., Mizzer, J.P., Thorpe, C., and Massey, V. (1982) Evidence that the greening ligand in native butyryl-CoA dehydrogenase is a CoA persulfide. *J Biol Chem* **257**: 4314–4320.
- Zhou, Y.-F., Nan, B., Nan, J., Ma, Q., Panjikar, S., Liang, Y.-H., et al. (2008) C4-dicarboxylates sensing mechanism revealed by the crystal structures of DctB sensor domain. *J Mol Biol* **383**: 49–61.
- Zoltowski, B.D., and Crane, B.R. (2008) Light activation of the LOV protein vivid generates a rapidly exchanging dimer. *Biochemistry* **47**: 7012–7019.
- Zoltowski, B.D., Schwerdtfeger, C., Widom, J., Loros, J.J., Bilwes, A.M., Dunlap, J.C., and Crane, B.R. (2007) Conformational switching in the fungal light sensor vivid. *Science* **316**: 1054–1057.

## Supporting information

Additional supporting information may be found in the online version of this article.

Please note: Wiley-Blackwell are not responsible for the content or functionality of any supporting materials supplied by the authors. Any queries (other than missing material) should be directed to the corresponding author for the article.